

1 **Linking temperature to catastrophe damages from hydrologic and meteorological**  
2 **extremes**

3

4 Conrad Wasko<sup>1,2</sup>, Ashish Sharma<sup>1</sup> and Alexander Pui<sup>3</sup>

5

6 <sup>1</sup> School of Civil and Environmental Engineering, University of New South Wales, Sydney,  
7 New South Wales, 2052, Australia

8 <sup>2</sup> Department of Infrastructure, University of Melbourne, Parkville, Victoria, 3010, Australia

9 <sup>3</sup> Swiss Re International Japan, Tokyo, Japan

10

11 **Abstract**

12 Increases in the magnitude of storm and flood related catastrophes due to climate change  
13 are predicted to increase associated economic losses. There exists, however, conflicting  
14 evidence for greater economic losses despite well acknowledged increases in the severity of  
15 observed extreme events in recent decades. Here, using a worldwide catastrophe insurance  
16 database from 1970 to 2015, we link the catastrophe economic loss from extreme storms  
17 and floods to local temperature. Although no statistically significant temporal trend is  
18 detected in standardised global catastrophe economic losses, we find a statistically  
19 significant positive association between economic losses expressed as a proportion of GDP  
20 and local temperature. The association between economic losses and temperature is  
21 greater as the event becomes more extreme, with the signal muted for flooding as  
22 compared to storms. Although local associations of economic loss with temperature cannot  
23 be directly linked to rising global temperatures as a result of climate change, the positive  
24 economic loss-temperature associations are consistent with observed extreme  
25 precipitation-temperature associations, and hence pertinent to the advancement of  
26 understanding future natural catastrophes.

27

28 **1. Introduction**

29 Storm related climate catastrophes result in major loss of life and widespread economic  
30 damage, with developing countries particularly exposed as they lack the financial and  
31 material resources to mitigate impacts (Razavi et al., 2020). Overall, the economic losses

32 from these catastrophes is expected to be exacerbated by climatic change (Arent et al.,  
33 2014; IPCC, 2012). This expectation is supported by evidence from dynamic downscaling of  
34 individual weather events and statistical downscaling of global climate models, both of  
35 which predict increased insurance losses can be expected as we head into the significantly  
36 warmer temperatures over the rest of this century (Held et al., 2013).

37

38 The contribution of climate change to economic loss potential from storm events is largely  
39 based on the assumption of increasing storm intensity driven via the Clausius-Clapeyron  
40 relation. Assuming constant relative humidity, this physical relationship dictates that as  
41 temperatures increase, so does the moisture holding capacity of the atmosphere, and hence  
42 extreme precipitation intensity should increase as a result (Trenberth, 2011; Trenberth et  
43 al., 2003). This in turn is predicted to lead to increased flood risk (Trenberth et al., 2003;  
44 Westra et al., 2014), particularly in urban settings (Fadhel et al., 2018; Hettiarachchi et al.,  
45 2018; Miller and Hutchins, 2017). Increases in precipitation intensity are likely to be coupled  
46 with changes in storm temporal pattern (Wasko and Sharma, 2015) as well as duration  
47 (Emmanuel et al., 2012; Webster, 2005) and areal extent (Prein et al., 2017). Storms may  
48 also invigorate due to increased latent heat release at higher (absolute) humidity  
49 intensifying upward motions (Lenderink and van Meijgaard, 2008; Trenberth et al., 2003), or  
50 change due to larger atmospheric changes such as the expansion of the Hadley Cell (Grise et  
51 al., 2018; Mathew and Kumar, 2019; Seidel et al., 2008; Staten et al., 2018) increasing the  
52 frequency of extreme precipitation events (Myhre et al., 2019). All these factors are  
53 predicted to lead to increased storm severity with climate change (Seneviratne et al., 2012).

54

55 Observed increases in extreme precipitation, flooding, and storm severity are abundant in  
56 literature (Do et al., 2017; Donat et al., 2013; Emanuel, 2005; Martinez-Villalobos and  
57 Neelin, 2018; O’Gorman, 2015; Slater et al., 2021; Sun et al., 2021; Wasko and Nathan,  
58 2019; Westra et al., 2013a). While historical changes in climate extremes have been  
59 attributed to anthropogenic climate change (Diffenbaugh et al., 2017; Kay et al., 2011; Min  
60 et al., 2011; Pall et al., 2011), the linking of economic losses to climatic change is more  
61 difficult (Bouwer, 2011; Hoeppe, 2016). Changes in economic losses have been associated  
62 with local climate variability (Pielke and Landsea, 1999; Welker and Faust, 2013), and the  
63 economic cost of hurricane Harvey has recently been attributed to climate change (Frame et

64 al., 2020), but debate remains on whether temporal trends in economic loss exist (Paprotny  
65 et al., 2018). Although a summary of historical studies finds more studies observe increases  
66 rather than decreases in economic loss (Bouwer, 2011), after appropriate normalisation for  
67 increases in economic growth, studies generally find little temporal trend and hence  
68 association with climate change (Arent et al., 2014). For example, normalised total annual  
69 losses from Hurricanes in the United States (Pielke et al., 2008; Weinkle et al., 2018) and  
70 Latin America and The Caribbean (Pielke et al., 2003) show no temporal trend. Likewise no  
71 climate change signal was identified in normalised annual aggregations of flood losses  
72 across Europe (Barredo, 2009).

73

74 Global normalised economic loss aggregations across various natural disaster types also  
75 display no statistically significant upward trend (Barthel and Neumayer, 2012; Neumayer  
76 and Barthel, 2011), with continental Australian studies showing similar results (Crompton  
77 and McAneney, 2008; McAneney et al., 2019). As global temperatures have been  
78 monotonically increasing and can be substituted for a temporal trend, there is likewise no  
79 link found between increasing global temperatures and increasing global economic losses  
80 (Miller et al., 2008). The two primary arguments for differing trends in economic loss are the  
81 method of normalisation of economic loss (Barthel and Neumayer, 2012; Kron et al., 2019)  
82 and the absence of consideration of changes in vulnerability (Mechler and Bouwer, 2015).  
83 For example, climate change signals may be obscured by increasing defences and resilience  
84 to climatic catastrophes (Nicholls, 2011) meaning increases in economic loss are not as large  
85 as they would have been had vulnerability-reducing measures not been implemented  
86 (Mechler and Bouwer, 2015). Here we suggest another possibility. As global warming does  
87 not always affect the global temperature uniformly (Neukom et al., 2019) it may be that  
88 higher global temperatures will not be associated with greater economic losses, but local  
89 temperatures will.

90

91 There is significant evidence that local temperature influences storm severity (Lenderink  
92 and van Meijgaard, 2008; Peleg et al., 2018). Changes in both tropical cyclones and local  
93 scale convective events have been correlated to increases in temperature (Lenderink and  
94 Attema, 2015; Webster, 2005). Increased lightning strikes have been linked to higher  
95 temperatures (Molnar et al., 2015) and a greater number of insurance claims (Mills, 2005).

96 Indeed, local temperature sensitivities have been shown to be the primary variable  
97 explaining rainfall variability across various temporal scales (Wasko and Sharma, 2017a;  
98 Westra et al., 2013b) with higher temperatures linked to greater flood event magnitude  
99 (Wasko and Sharma, 2017b). Local temperature increases have been successfully used as a  
100 predictor in non-stationary analysis of flood risk (Condon et al., 2015; Towler et al., 2010)  
101 and extreme rainfall (Agilan and Umamahesh, 2015; Mondal and Mujumdar, 2015), even  
102 being linked to indicators of water quality (Guo et al., 2021) and hence health outcomes  
103 (Jhajharia et al., 2013).

104

105 As discussed above, storm extremes are linked to higher temperatures from the increased  
106 moisture carrying capacity of a warmer atmosphere as specified by the Clausius Clapeyron  
107 relationship (Roderick et al., 2019; Trenberth, 2011). Assuming constant relative humidity,  
108 this increase in moisture carrying capacity can lead to larger downpours especially over  
109 short periods of time where local moisture contributes substantially (Fowler et al., 2021).  
110 While this physical link to temperature becomes weaker when the relationship is extended  
111 to other derived variables such as floods (Bennett et al., 2018; Sharma et al., 2018; Trambly  
112 et al., 2019) and economic loss (Nicholls, 2011), a positive link with extreme precipitation is  
113 well established. Hence, here we seek to investigate, can a link between temperature and  
114 the economic loss resulting from extreme hydrologic and meteorological events be  
115 identified?

116

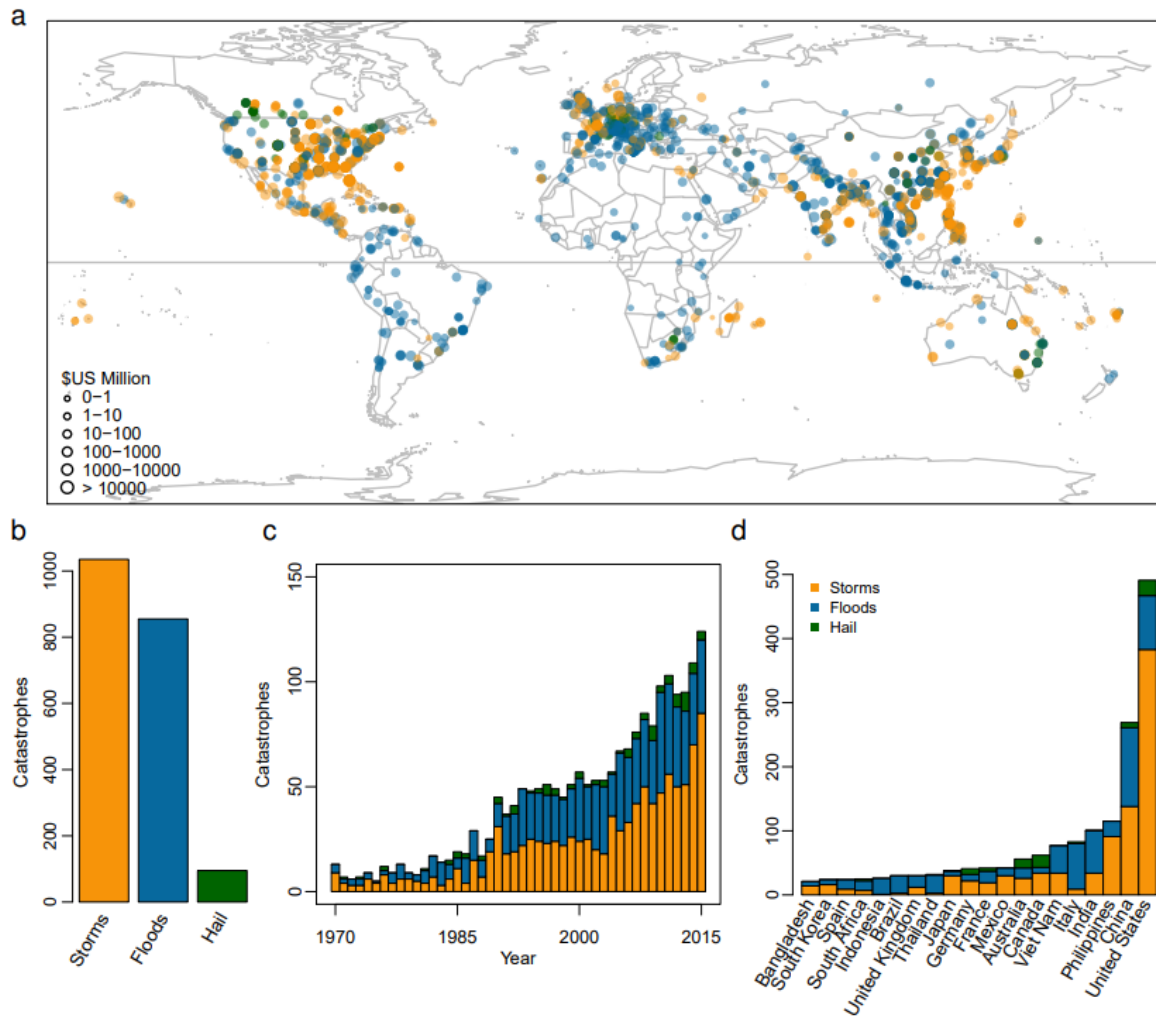
117 We analyse natural disasters on a per event basis, rather than a total or annual economic  
118 loss, to capture the event severity (in terms of economic loss). The normalised temporal  
119 trend on a per catastrophe basis is first analysed to see if economic losses have increased  
120 due to an increase in event severity. Next, because global temperature anomalies are not  
121 necessarily spatially uniform, the sensitivity of normalised economic loss to local  
122 temperature as a driver of storm intensification is investigated. The influence of storm  
123 severity and the originating storm mechanism on the relationship of normalised economic  
124 loss to local temperature are also investigated. Finally, the implications in the context of  
125 climate change are discussed.

126

127 **2. Data**

128 In this study we use the Sigma catastrophe database for the years 1970 to 2015 (SwissRe,  
129 2016). Sigma represents a comprehensive database of significant catastrophe events  
130 collated from newspapers, direct and reinsurance periodicals, specialist publications and  
131 reports from (re)insurers. This data set provides information on 5024 natural catastrophes  
132 for which various statistics are reported including fatalities, economic loss, and insured loss.  
133 Here, we focus on the economic loss. The economic loss consists of both infrastructure  
134 damage (stock losses) and lost production due to economic interruption (flow losses). The  
135 total economic loss is reported as: A nominal loss in the local currency; the local loss in U.S.  
136 dollars; and the inflated loss in 2016 U.S. dollars. The nominal economic loss is converted to  
137 U.S. dollars using the end of year exchange rate and subsequently the U.S. dollar value is  
138 adjusted for inflation using the US consumer price index to give economic loss for the base  
139 year 2016. Consistent with insurance industry practice, catastrophes are classified on the  
140 type of catastrophe using peril terminology. These perils are storms, floods, hail, heat  
141 related catastrophes such as droughts and fires, cold related catastrophes such blizzards,  
142 earthquakes, or unclassified. Storm damages generally stem from events causing water  
143 ingress or wind driven rain damage whereas flood events are generally from riverine  
144 inundation such as over topping of riverbanks. Perils originating from blizzards can be  
145 classified as either cold related catastrophes or storms depending on the primary peril. A  
146 description of each event is also given providing the storm mechanism. For example, the  
147 Haiyan typhoon of 2013 in the Philippines is classified as a storm and described as “Haiyan  
148 typhoon”. Such data sets provide a quantitative link between the hydrologic sciences and  
149 economic loss (Gao et al., 2019).

150



151  
 152 *Figure 1. Economic loss data. (a) Inflated economic loss per catastrophe. The size of the circle*  
 153 *indicates the size of the economic loss in 2016 US million dollars. The colour of the circle indicates the*  
 154 *type of peril. (b) Histogram of catastrophe number. (c) Time series of catastrophe number. (d)*  
 155 *Histogram of catastrophe country origin for countries with more than 20 recorded catastrophes.*

156  
 157 Here we focus on the hydrologic storm related catastrophes, that is storms, floods, or hail  
 158 events, a total of 1985 events. The location of each catastrophe is reported as a region,  
 159 state, territory, or country. For this study the location description was mapped to  
 160 geographical coordinates using an application programming interface. The location and  
 161 economic loss of each catastrophe is presented in Figure 1a. Economic loss is highly non-  
 162 linear with the largest 50% of events responsible for 97% of losses, and the largest 10%  
 163 responsible for 75% of losses, after normalisation (Section 3.1). The automated matching of  
 164 each catastrophe event to a set of coordinates was verified manually. The proportion of  
 165 catastrophes classified as either storms or floods far exceeds those classified as hail (Figure

166 1b). The number of recorded events has increased in time (Figure 1c), with few recorded  
167 events prior to 1985. For countries with more than 20 recorded catastrophes, the number of  
168 catastrophes is summarised in Figure 1d. Most recorded events are in the Unites States,  
169 Europe, and China (Figure 1a, 1d).

170

### 171 **3. Methods**

#### 172 **3.1 Normalisation of individual catastrophes**

173 We analyse economic loss on a per catastrophe basis to isolate possible increases in storm  
174 severity. The effect of normalisation on economic loss is discussed in detail in Neumayer and  
175 Barthel (2011). For spatial pooling, for a given catastrophe year ( $t$ ), normalising by the  
176 country wealth is recommended (Neumayer and Barthel, 2011):

177

$$178 \quad y_i = \text{Normalised Economic Loss}_i = \frac{\text{Economic Loss}_i^t}{\text{Wealth}^t} \quad (1)$$

179

180 This results in a sample of normalised economic loss  $y_i$  where  $i = 1..n$  and  $n$  is the total  
181 number of events (as presented in Figure 1a). As long as the wealth is for the same year as  
182 the economic loss, the result is a dimensionless ratio of the actual loss to the potential loss  
183 (APLR) which can then be pooled spatially (Neumayer and Barthel, 2011). As discussed,  
184 economic loss consists of both losses to physical infrastructure (stock) and losses related to  
185 economic losses (flow). To accurately normalise a measure of wealth is required. A  
186 simplification is to use GDP as a wealth measure. Although GDP is a flow measure, it is  
187 typically highly correlated with wealth stock (Neumayer and Barthel, 2011) resulting in  
188 consistent normalisations (Paprotny et al., 2018). Here, the nominal Gross Domestic Product  
189 in U.S. dollars (UN, 2017) is used as an indicator of wealth consistent with standard practice  
190 (Munich RE, 2016) and previous studies (Neumayer and Barthel, 2011; Pielke and Landsea,  
191 1999; Welker and Faust, 2013). Twelve catastrophes with a normalised economic loss (APLR)  
192 above 0.4 were removed. These catastrophes were for small nations where the normalised  
193 economic loss is improbably high (Neumayer and Barthel, 2011). Removal of these data  
194 points did not affect the results presented.

195

#### 196 **3.2 Analysis of temporal trend**

197 For temporal analysis, the total normalised economic loss for each calendar year is divided  
 198 by the number of catastrophes recorded to find the average normalised economic loss per  
 199 catastrophe. The temporal trend of normalised economic loss per catastrophe per year was  
 200 assessed using the non-parametric rank-based Kendall's Tau correlation (Kendall, 1975,  
 201 1938). Kendall's Tau is a rank-based (non-parametric) correlation measure which equals 1 if  
 202 all pairs are concordant and -1 if all pairs are discordant (Equation 2).

$$203 \quad \tau = \frac{N_c - N_d}{n(n-1)/2} \quad (2)$$

204 Where  $N_c$  and  $N_d$  are the number of concordant discordant pairs respectively and  $n$  is the  
 205 number of observations, in this case years. The temporal trend was calculated with a varying  
 206 start and end year ensuring that the minimum record length considered was 10 years. This  
 207 allowed consideration of change points or bias due to an individual year or short period  
 208 having a high normalised economic loss. Due to the possibility of serial autocorrelation it is  
 209 prudent to use multiple trend tests (Zamani et al., 2017). The analysis was repeated using a  
 210 modified Mann-Kendall test with bias corrected pre-whitening to remove the effect of any  
 211 serial correlation (Hamed, 2009). As the results were consistent with those based on  
 212 Kendall's Tau the results presented here focus on the use of Kendall's Tau.

213

### 214 **3.3 Analysis of temperature associations**

215 The Clausius-Clapeyron equation describes how the equilibrium vapour pressure ( $e_s$ ) varies  
 216 with Temperature ( $T$ ):

$$217 \quad \frac{\partial e_s}{\partial T} \simeq \frac{e_s L_v(T)}{R_v T^2} \quad (3)$$

218 where  $L_v$  is the latent heat of vapourisation and  $R_v$  is the gas constant. As temperature  
 219 increases, the saturation vapour pressure increases exponentially translating to an increase  
 220 between 5.7-6.7%/°C in the range 10-30°C (Wasko, 2021). Hence the intensity (and severity)  
 221 of an extreme storm event can be linked to local temperature (Agilan and Umamahesh,  
 222 2017; Fowler et al., 2021; Lenderink and Attema, 2015).

223 Here, each standardised catastrophe event was matched to the local NCEP/NCAR  
 224 Reanalysis 1 monthly temperature on a 2.5° grid (Kalnay et al., 1996; NCEP, 1994) based on  
 225 the start time of the catastrophe. Monthly temperature was used as it has been shown be an  
 226 effective predictor for non-stationary flood risk (Condon et al., 2015; Towler et al., 2010) and

227 extreme rainfall intensities (Agilan and Umamahesh, 2015; Cross et al., 2020; Wasko and  
 228 Sharma, 2017a). The analysis was also performed using an observed  $1.0^\circ$  gridded dataset  
 229 (Berkeley Earth, 2015; Rohde et al., 2013) with the results found to be almost identical. All  
 230 the standardised catastrophe events (Equation 1), with their matched local temperature,  
 231 were pooled and their sensitivity (association) to temperature was investigated using  
 232 quantile regression (Koenker and Bassett, 1978; Wasko and Sharma, 2014). Quantile  
 233 regression was implemented in the statistical software *R* using the package ‘quantreg’  
 234 (Koenker, 2021). Quantile regression allows the response with differing event rarity to be  
 235 investigated and is less biased to outlying data. A quantile regression is fitted to the  
 236 logarithm of economic loss.

237 Quantile regression is similar to linear regression and is expressed as per Equation (4) but a  
 238 cost function  $D$  is used to minimize deviation from the quantile ( $q$ ) of interest (Equation 5).  
 239 That is, for a regression of the form where  $y_i$  is the normalised economic loss for each  
 240 catastrophe and  $T_i$  is the local monthly temperature:

$$241 \quad \log(y_i) = \beta_0^{(q)} + \beta_1^{(q)}T_i \quad (4)$$

242 The regression coefficients  $\beta_0^{(q)}$  and  $\beta_1^{(q)}$  are chosen to minimize a cost function  $D$ , defined  
 243 as:

$$244 \quad D(\beta_0^{(q)}, \beta_1^{(q)}) = q \sum_{y_i \geq \beta_0^{(q)} + \beta_1^{(q)}T_i} |y_i - \beta_0^{(q)} - \beta_1^{(q)}T_i| + (1 - q) \sum_{y_i < \beta_0^{(q)} + \beta_1^{(q)}T_i} |y_i - \beta_0^{(q)} - \beta_1^{(q)}T_i| \quad (5)$$

246 For example, to regress for the 99<sup>th</sup> percentile,  $q$  is set equal to 0.99 and substituted into  
 247 Equation (5) to calculate the regression coefficients  $\beta_0^{(0.99)}$  and  $\beta_1^{(0.99)}$ . This substitution  
 248 results in a large weight for the first summation term (points above the regression line) and  
 249 a small weight for the second summation term (points below the regression line) resulting in  
 250 regression coefficients being optimised to minimise the absolute difference of fitted values  
 251 close to the first summation term, that is, the fitted regression line to the 99<sup>th</sup> percentile of  
 252 all the data.

253

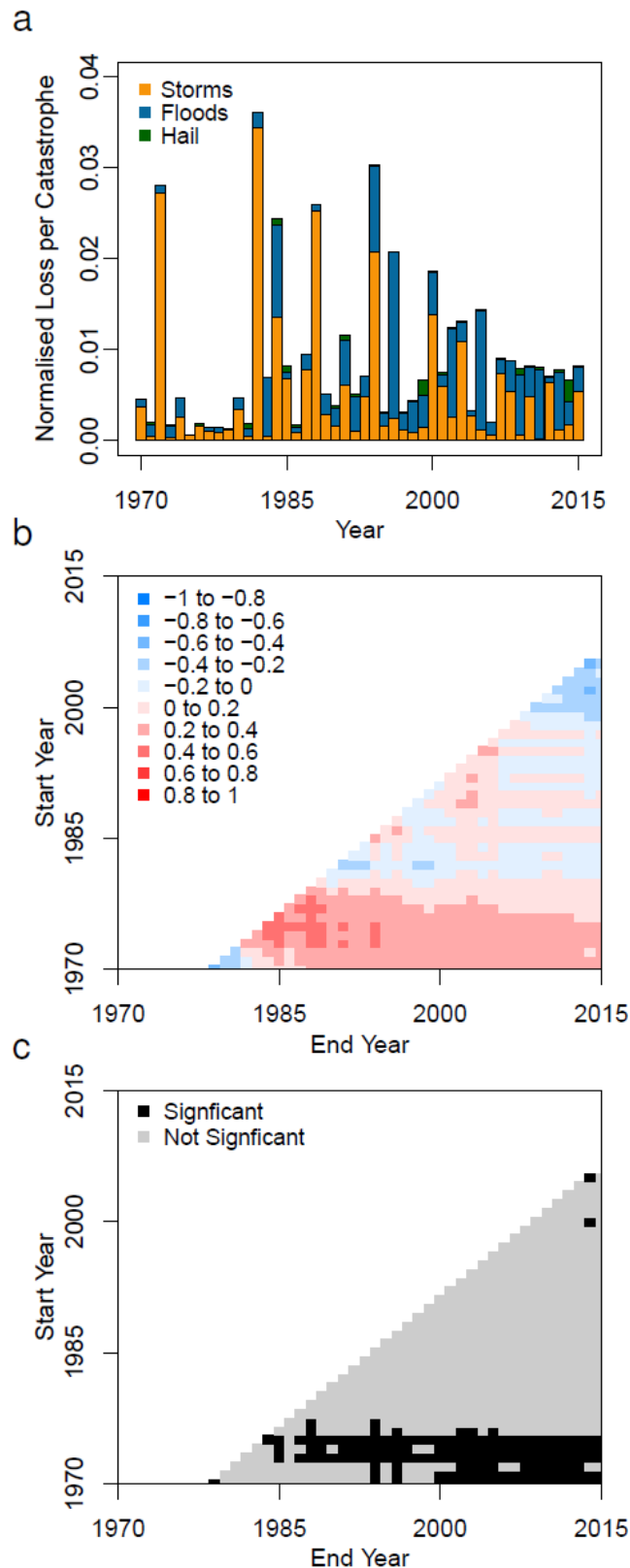
254 The sensitivity of the normalised economic loss ( $y$ ) as a percentage change per degree in  
255 temperature is then calculated by:

$$256 \quad \Delta y\% = 100 \cdot (10^{\beta_1} - 1) \quad (6)$$

257

258 As China and the U.S. account for almost 40% of our catastrophe sample (Figure 1d), and  
259 have the two largest global Gross Domestic Products, the catastrophe data is split between  
260 these two countries and those remaining to prevent possible bias due to the uneven sample  
261 of events between countries. Individual quantiles were calculated using a 2°C moving  
262 temperature window to confirm the assumption of linearity between the logarithm of  
263 normalised economic loss and temperature. To analyse the possible impact of storm  
264 mechanism each event description was mined for key words. These were  
265 tornado/thunderstorm, hurricane, typhoon, and cyclone/tropical storm. Descriptions  
266 without these key words were classified as 'other' storms and include storms described as  
267 winter storms as well as storms without any additional description. The temperature range  
268 used for regression (to remove the influence of outliers) is indicated in each figure by the  
269 extents of the fitted regression.

270



271

272 *Figure 2. Per catastrophe trend analysis (a) Economic loss per catastrophe per year standardised by*

273 *GDP. (b) Surface of Kendall's tau statistic for monotonic trend in Figure 2a. Kendall's tau has been*

274 *calculated on a time series from the start year to the end year with a minimum record length of 10*

275 *years. (c) Statistical significance of Kendall's tau presented in Figure 2b at the 95% level.*

276 **4. Results**

277 **4.1 Temporal trend**

278 A time series of the normalised economic loss per catastrophe per year is presented in  
279 Figure 2a. For simplicity, from here on, economic loss refers to the economic loss  
280 standardised by GDP. A surface of Kendall's tau statistic for monotonic trend is presented in  
281 Figure 2b. Statistical significance is presented in Figure 2c. The trend test is performed on a  
282 moving window of years, with a minimum of 10 years required for testing. Economic loss  
283 per catastrophe is seen to increase only if the data pre-1980 is included but there is minimal  
284 catastrophe data recorded before 1985 (Figure 1c). When data pre-1980 is omitted no  
285 statistically significant trends are obtained. These results are consistent with previous global  
286 studies that used annual aggregations (rather than the per event analysis performed here)  
287 that concluded there is little evidence for a temporal increase in catastrophe related  
288 economic loss (Miller et al., 2008; Neumayer and Barthel, 2011).

289

290 **4.2 Sensitivity to temperature**

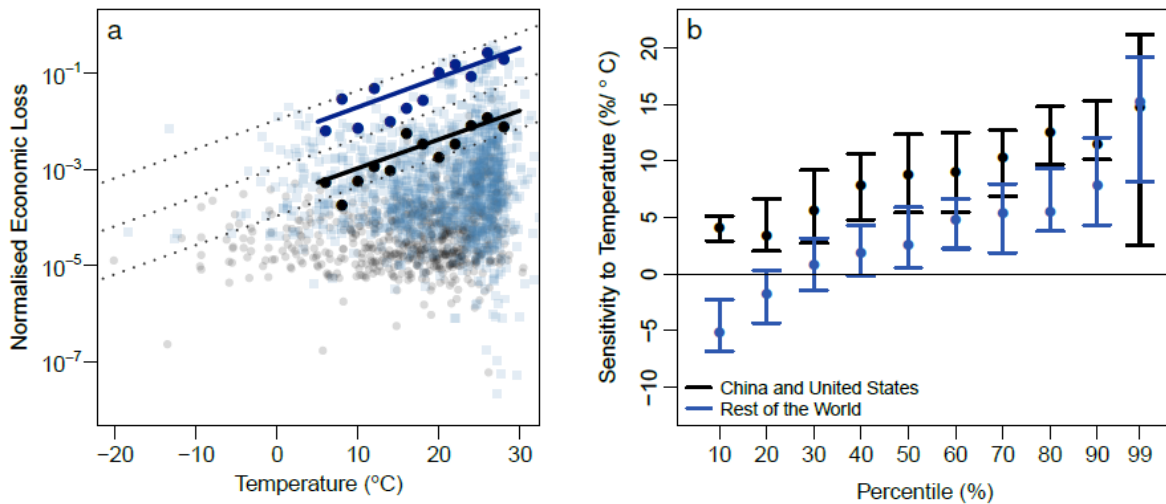
291 The economic loss as a function of local temperature is presented in Figure 3a. The trend  
292 lines were fitted using quantile regression for the 99<sup>th</sup> percentile. To confirm linearity the  
293 points present the 99<sup>th</sup> percentile calculated empirically from the data using a moving  
294 temperature window. The economic loss for China and the U.S. exhibit a sensitivity of  
295 14.8%/°C, with the rest of the world demonstrating a sensitivity of economic loss to  
296 temperature of 15.2%/°C. We note the analysis was also performed repeated using an  
297 observed gridded temperature product (Berkeley Earth, 2015; Rohde et al., 2013) and the  
298 results were found to be consistent with those presented in Figure 3a.

299

300 The most extreme percentiles have the greatest sensitivity to temperature with less  
301 extreme catastrophes less sensitive to higher temperature (Figure 3b). The median  
302 catastrophe economic loss sensitivity to temperature is 8.8%/°C for the U.S. and China, and  
303 2.6%/°C for the rest of the world. Using panel regression gave similar results (not shown).  
304 Below the median there is evidence of a negative association between economic loss and  
305 temperature when the U.S. and China are excluded. The positive associations with  
306 temperature for both China and U.S. and the rest of the world are similar and within  
307 confidence limits for the most extreme percentiles. The sensitivities of economic loss with

308 temperature are consistent with observed increased storm severity with higher  
 309 temperatures (Webster, 2005), with this association stronger the more extreme the event  
 310 (Wasko and Sharma, 2017b).

311



312

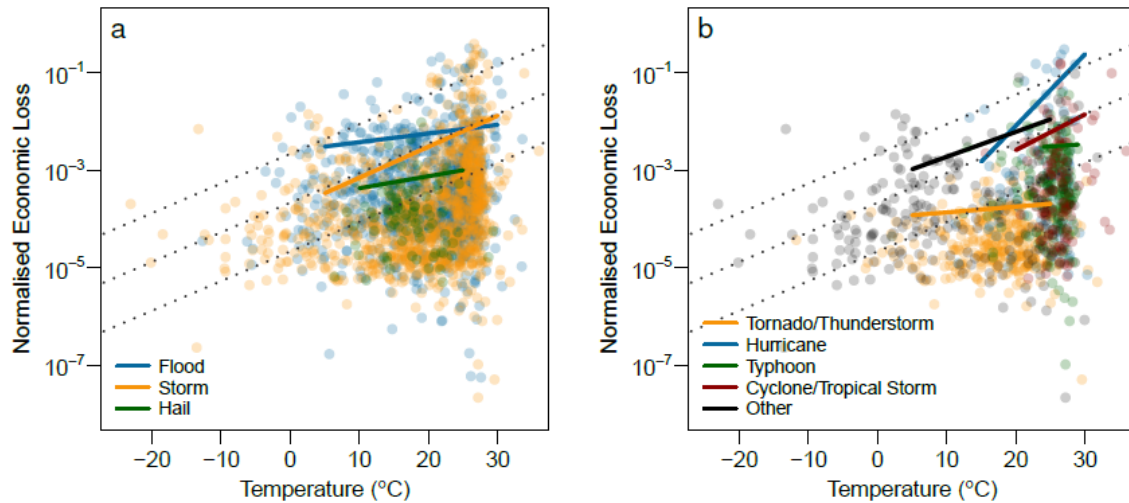
313 *Figure 3. Relationship between economic loss, temperature, and percentile for global*  
 314 *catastrophe data (a) Relationship between economic loss and temperature. Data is analysed*  
 315 *between 5 and 30°C to avoid influence of outlying data. Filled circles show the 99<sup>th</sup>*  
 316 *percentile for moving 2°C temperature bins. The straight lines are the quantile regression*  
 317 *fitted to the logarithm of economic loss for the 99<sup>th</sup> percentile. Dotted guidelines show a*  
 318 *sensitivity of 15% per °C. (b) Sensitivity of economic loss - temperature relationship to*  
 319 *percentile. The whiskers are the 95% confidence interval of the fitted quantile regression for*  
 320 *the target percentile.*

321

### 322 4.3 Variability with peril

323 The 90<sup>th</sup> percentile sensitivity of economic loss to temperature for each individual peril  
 324 (flood, storm, hail), using all the data presented in Figure 3a, is presented in Figure 4a. The  
 325 sensitivities and their statistical significance are summarised in Table 1. There are few  
 326 catastrophes classified as hail (Figure 1b) and hence the sensitivity of hail economic loss  
 327 with temperature (5.8%/°C) is not statistically significant (Table 1). However, it appears that  
 328 storm economic loss has a greater (more positive) sensitivity to temperature (15.8%/°C)  
 329 than the economic loss from flooding (4.2%/°C). This is consistent with drier soil moisture

330 conditions at higher temperature reducing the sensitivity of floods to higher temperature  
 331 (Ivancic and Shaw, 2015; Wasko et al., 2019; Wasko and Nathan, 2019).  
 332



333  
 334 *Figure 4. Dependence of economic loss sensitivity to temperature depending on peril type*  
 335 *and storm mechanism. (a) Sensitivity of economic loss to temperature for peril classifications*  
 336 *of flood, storm, and hail. (b) Sensitivity of economic loss to temperature for storm*  
 337 *catastrophes classified as a tornado, hurricane, typhoon, cyclone and unclassified (other). All*  
 338 *fitted lines are for the 90<sup>th</sup> percentile quantile regression. Guidelines show sensitivity of 15%*  
 339 *per °C. Table 1 presents sensitivities and p-values for each regression.*

340  
 341 The storm data is subdivided further by storm mechanism (Figure 4b). Although hurricanes,  
 342 typhoons, and cyclones are a result of similar weather phenomena, as they originate in  
 343 different climatic regions they are classified separately to remove artefacts of spatial  
 344 pooling. Indeed catastrophes such as hurricanes, typhoons, and cyclones are associated with  
 345 higher temperatures (sit towards the right of the figure), possibly due to originating in the  
 346 tropics where temperatures are warmer. Additionally, the economic loss for these  
 347 catastrophes is much greater than those classified as thunderstorms. Hence, a mixing of  
 348 storm mechanisms may have introduced an artefact in the pooled analysis of storms, with  
 349 the positive association in temperature due to sampling different storm types originating  
 350 from different locations. For each of the individual storm classifications a positive  
 351 association between economic loss and temperature is still observed suggesting greater  
 352 storm severity and economic loss with higher temperatures regardless of storm mechanism

353 (and location). However, the statistical significance of these associations is less due to the  
 354 smaller sample sizes (Table 1).

355

356 *Table 1. Summary of economic loss-temperature sensitivities presented in Figure 4 and their*  
 357 *statistical significance.*

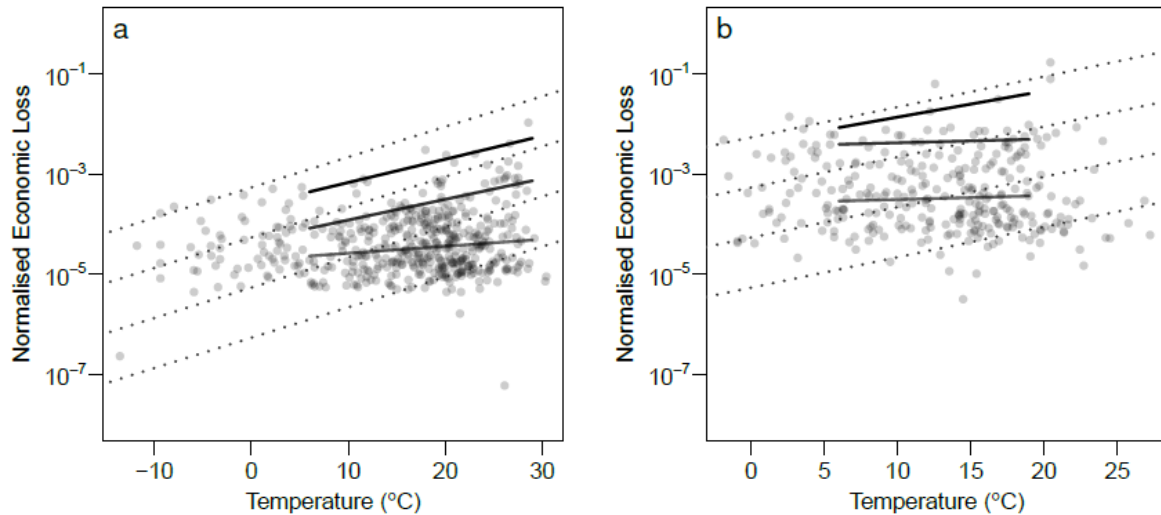
Classification Class	Classification	Sensitivity (% per °C)	p-value
Peril	Flood	4.2	0.07
	Storm	15.8	0.00
	Hail	5.8	0.68
Storm type	Tornado/Thunderstorm	2.7	0.31
	Hurricane	40.2	0.05
	Typhoon	2.3	0.90
	Cyclone/Tropical Storm	18.3	0.38
	Other	12.5	0.04

358

#### 359 **4.4 Validity of spatial pooling**

360 It is prudent to address the validity of normalisation by conducting an analysis without  
 361 pooling across the global scale. A sensitivity test using only data for the U.S. is presented in  
 362 Figure 5a. The results are consistent with global trends (Figure 3) suggesting the global  
 363 pooling results in a homogenous economic loss data set. When the results at a continental  
 364 scale, for example Europe, are investigated, the sensitivities are subdued (Figure 5b). The  
 365 99<sup>th</sup> percentile continues to display a sensitivity of approximately 15%/°C consistent with  
 366 global results (Figure 3a), but the median displays a sensitivity of 2%/°C. This is not  
 367 surprising given the mixed signal in flooding throughout Europe and small data size (Blöschl  
 368 et al., 2017; Hall et al., 2014). In context with the results presenting sensitivity to storm  
 369 mechanism (Figure 4), this suggests that local and regional climatic conditions (Pielke and  
 370 Landsea, 1999; Welker and Faust, 2013) need to be considered, as trends in extreme events  
 371 can be mixed (Mallakpour and Villarini, 2015; Wasko, 2021) and also affected by the  
 372 uncertainty in extreme value analysis (Hall et al., 2014). However, repeating the results  
 373 classifying on storm mechanism just for the U.S., our largest economically homogenous  
 374 sample, also showed positive associations with temperature for storms identified as  
 375 tornado/thunderstorm or hurricane (not shown).

376



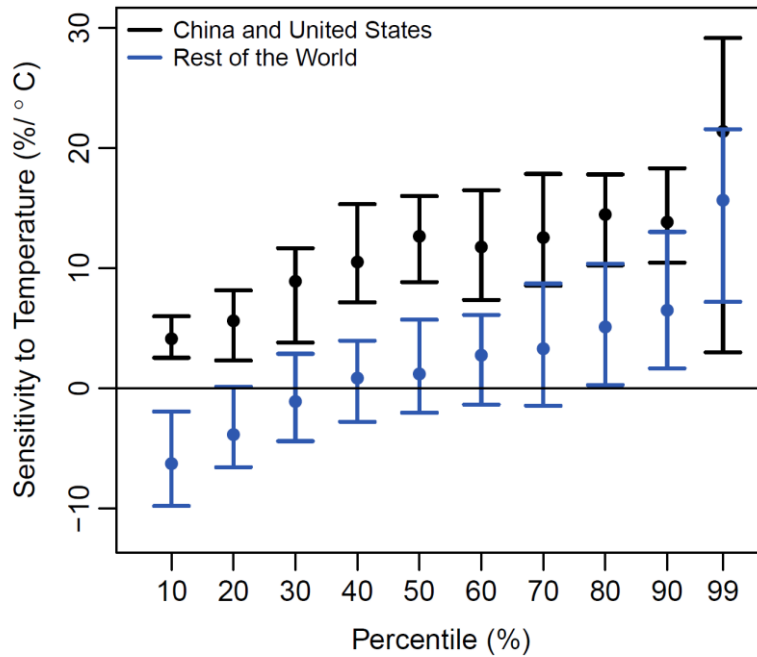
377

378 *Figure 5. Sensitivity of economic loss to temperature (a) United States (b) Europe. The solid lines are*  
 379 *quantile regressions for the 50th, 90th and 99th percentiles in increasing opacity. Guidelines show a*  
 380 *sensitivity of 15% per °C. Trends presented for Europe are not significantly different from zero. Trends*  
 381 *presented for the United States are significantly different from zero. Significance was tested at the*  
 382 *95% level.*

#### 383 **4.5 Confounding due to unequal sampling**

384 Increased temperatures in recent years may correlate with recent catastrophes which are  
 385 sampled with greater frequency (Figure 1c) inducing a positive sensitivity, though this is  
 386 unlikely as previous studies have not found a trend with temperature anomalies at the  
 387 global scale (Miller et al., 2008). Figure 6 presents the results shown in Figure 3b with data  
 388 resampled to ensure that the number of catastrophes per year is a constant 20 events per  
 389 year. This removes possible bias associated with the number of events being skewed to  
 390 more recent, warmer, years. The results of resampling are consistent with the positive  
 391 sensitivity of economic losses with temperature for extreme percentiles presented earlier  
 392 (Figure 3) meaning the results presented here are not an artefact of sampling more recent  
 393 (warmer) events.

394



395

396 *Figure 6. Resampled sensitivity of economic loss to temperature with percentile. Resampling is*  
 397 *performed on data post 1990, sampling an equal 20 events for each year. Whiskers are 95%*  
 398 *confidence intervals estimated from a bootstrap of 1000 replicates.*

399 **5. Discussion**

400 Historical trends in economic loss are often investigated, and an identification of such a  
 401 trend attributed to climatic change due to the historically increasing greenhouse gasses  
 402 increasing temperatures and changing atmospheric circulations. It is hence common  
 403 practice, and entirely valid, to substitute historical global temperature anomalies for the  
 404 temporal trend as both are strongly correlated. But this practice is not necessarily  
 405 informative of changes to damage due to changed storm intensity, as storm intensity is  
 406 correlated to the absolute temperature and not anomalies as per Equation 3. For this  
 407 reason, we associated local temperature with the economic cost of a catastrophic event.  
 408 Despite changes in local temperature having better predictive ability of extreme rainfalls  
 409 than temporal trends (Agilan and Umamahesh, 2015, 2017; Mondal and Mujumdar, 2015),  
 410 and historical trends in extreme rainfall severity showing a strong similarity to historical  
 411 temperature increases (Sun et al., 2021; Wasko and Nathan, 2019; Zhang et al., 2019) there  
 412 is significant discussion in the literature on whether day-to-day variability is representative  
 413 of a meaningful (temporal) physical relationship (Wasko, 2021; Zhang et al., 2017).

414

415 For example, there is no guarantee that a global temperature anomaly is experienced  
416 universally with global warming. Global warming differs by season and latitude, with the  
417 largest warming in winter and in high-latitudes (e.g., the coldest climates). Hence, it may be  
418 that the local temperature associations presented here are coupled with this trend, though  
419 stratifying on region continued to show consistent positive associations with temperature,  
420 suggesting this is not the case. There is also the issue of mixing ‘weather’ types (Haerter and  
421 Berg, 2009; Magan et al., 2020; Molnar et al., 2015; Wasko et al., 2015) where different  
422 weather events originate in different regions and at different temperatures (Section 4.3)  
423 which can alias to induce a positive signal between storm intensity and temperature.  
424 Separating out the mixing of events, such as hurricanes which originate in warmer areas,  
425 positive associations with temperature for each individual weather type were still found  
426 (Figure 4b), with the results consistent with modelled intensification of hurricane Harvey  
427 (van Oldenborgh et al., 2017). Catastrophes that were not been attributed to a storm  
428 mechanism (labelled ‘other’) were presented in black (Figure 4b). It is not known whether  
429 these storms have simply not been classified and hence may be a mix of the existing  
430 classifications or are a mix of storms of varying sizes with a similar storm mechanism.  
431 However, the economic loss associated with these storms does exhibit a sensitivity with  
432 temperature at a rate of approximately 12.5%/°C consistent with greater storm severity at  
433 higher temperatures.

434

435 The originating season of weather event has also been suggested as a confounding factor  
436 with temperature associations suggested to be a function of seasonality (Zhang et al., 2017).  
437 The data presented in Figure 3a was also stratified on season and showed consistent  
438 positive sensitivities. Despite our best efforts to remove any artefacts, there remains a  
439 possibility that due to pooling across space, positive associations of temperature and  
440 economic loss are due to economic loss event mechanisms generally originating from  
441 climates with higher temperatures. However, even if this was to be true, a shift to the more  
442 intense storm mechanisms associated with higher temperatures is not inconsistent with  
443 climate change (Berg et al., 2013). For example, the poleward shifts of the tropics is likely to  
444 bring with it changing weather types (Grise et al., 2018; Seidel et al., 2008; Staten et al.,  
445 2018) and increased tropical cyclone activity (Daloz and Camargo, 2018).

446

447 Finally, it needs to be noted that linearity was assumed between the logarithm of  
448 standardised economic loss and temperature. This was verified by plotting the empirical  
449 percentiles (Figure 2) but there is no guarantee that this linearity will exist beyond the  
450 temperature ranges presented here, or in the future, if the changes in weather patterns are  
451 outside those that can be captured by assuming linearity. In the absence of better evidence  
452 we continued with the assumption of linearity in this manuscript but note flood damage  
453 functions can take many function forms (Li et al., 2016).

454

## 455 **6. Conclusions**

456 Previous studies that have attempted to link economic loss with temperature anomalies at a  
457 global scale did not find a historical trend in economic loss. Here, we investigated the  
458 sensitivity (association) of catastrophe loss with local temperature on a per catastrophe  
459 basis. Consistent with existing literature, we found little evidence for increased economic  
460 loss in time due to storms increasing in severity. However, we did find higher local  
461 temperatures are associated with greater economic loss. The positive association is  
462 commensurate with the intensity of the event, that is, the more extreme the catastrophe,  
463 the more positive the association. This is consistent with the physical reasoning of greater  
464 storm intensity and severity at higher temperatures, and historical trends of increased  
465 severity of precipitation and flood extremes with climate change.

466

467 The focus here was on catastrophe severity and not the frequency of catastrophes. If  
468 catastrophe frequency was to increase (Mallakpour and Villarini, 2015; Molnar et al., 2015)  
469 then economic losses as an aggregation could be expected to increase also (Held et al.,  
470 2013; Mills et al., 2002). It is likely that both greater storm intensities at higher  
471 temperatures, and, an increased sampling of more catastrophic storm types such as  
472 hurricanes (originating at higher temperatures), result in the positive association of  
473 economic losses and local temperatures observed here. Although our analysis cannot be  
474 directly linked to rising global temperatures as a result of climate change the results suggest  
475 any possible future shift in storm type with higher temperatures, coupled with increasing  
476 storm severity, may further exacerbate economic losses from natural catastrophes.

477

478

479 **Acknowledgments**

480 Conrad Wasko receives funding from the University of Melbourne McKenzie Postdoctoral  
481 Fellowship scheme and Australian Research Council (DE210100479, DP200101326).

482

483 **References**

484 Agilan, V., Umamahesh, N.V., 2015. Detection and attribution of non-stationarity in intensity  
485 and frequency of daily and 4-h extreme rainfall of Hyderabad, India. *J. Hydrol.* 530,  
486 677–697. <https://doi.org/10.1016/j.jhydrol.2015.10.028>

487 Agilan, V., Umamahesh, N. V., 2017. What are the best covariates for developing non-  
488 stationary rainfall Intensity-Duration-Frequency relationship? *Adv. Water Resour.* 101,  
489 11–22. <https://doi.org/10.1016/j.advwatres.2016.12.016>

490 Arent, D.J., Tol, R.S.J., Faust, E., Hella, J.P., Kumar, S., Strzepek, K.M., Tóth, F.L., Yan, D.,  
491 2014. Key economic sectors and services, in: *Climate Change 2014: Impacts,*  
492 *Adaptation, and Vulnerability. Part A: Global and Sectoral Aspects. Contribution of*  
493 *Working Group II to the Fifth Assessment Report of the Intergovernmental Panel on*  
494 *Climate Change.* pp. 659–708. <https://doi.org/10.1017/CBO9781107415379.015>

495 Barredo, J.I., 2009. Normalised flood losses in Europe: 1970–2006. *Nat. Hazards Earth Syst.*  
496 *Sci.* 9, 97–104. <https://doi.org/10.5194/nhess-9-97-2009>

497 Barthel, F., Neumayer, E., 2012. A trend analysis of normalized insured damage from natural  
498 disasters. *Clim. Change* 113, 215–237. <https://doi.org/10.1007/s10584-011-0331-2>

499 Bennett, B., Leonard, M., Deng, Y., Westra, S., 2018. An empirical investigation into the  
500 effect of antecedent precipitation on flood volume. *J. Hydrol.* 567, 435–445.  
501 <https://doi.org/10.1016/j.jhydrol.2018.10.025>

502 Berg, P., Moseley, C., Haerter, J.O., 2013. Strong increase in convective precipitation in  
503 response to higher temperatures. *Nat. Geosci.* 6, 181–185.  
504 <https://doi.org/10.1038/ngeo1731>

505 Berkeley Earth, 2015. Berkeley Earth Project. [available at <http://berkeleyearth.org/data/>].

506 Blöschl, G., Hall, J., Parajka, J., Perdigão, R.A.P., Merz, B., Arheimer, B., Aronica, G.T.,  
507 Bilibashi, A., Bonacci, O., Borga, M., Čanjevac, I., Castellarin, A., Chirico, G.B., Claps, P.,  
508 Fiala, K., Frolova, N., Gorbachova, L., Gül, A., Hannaford, J., Harrigan, S., Kireeva, M.,  
509 Kiss, A., Kjeldsen, T.R., Kohnová, S., Koskela, J.J., Ledvinka, O., Macdonald, N., Mavrova-  
510 Guirguinova, M., Mediero, L., Merz, R., Molnar, P., Montanari, A., Murphy, C., Osuch,

511 M., Ovcharuk, V., Radevski, I., Rogger, M., Salinas, J.L., Sauquet, E., Šraj, M., Szolgay, J.,  
512 Viglione, A., Volpi, E., Wilson, D., Zaimi, K., Živković, N., 2017. Changing climate shifts  
513 timing of European floods. *Science* (80- ). 357, 588–590.  
514 <https://doi.org/10.1126/science.aan2506>

515 Bouwer, L.M., 2011. Have Disaster Losses Increased Due to Anthropogenic Climate Change?  
516 *Bull. Am. Meteorol. Soc.* 92, 39–46. <https://doi.org/10.1175/2010BAMS3092.1>

517 Condon, L.E., Gangopadhyay, S., Pruitt, T., 2015. Climate change and non-stationary flood  
518 risk for the upper Truckee River basin. *Hydrol. Earth Syst. Sci.* 19, 159–175.  
519 <https://doi.org/10.5194/hess-19-159-2015>

520 Crompton, R.P., McAneney, K.J., 2008. Normalised Australian insured losses from  
521 meteorological hazards: 1967-2006. *Environ. Sci. Policy* 11, 371–378.  
522 <https://doi.org/10.1016/j.envsci.2008.01.005>

523 Cross, D., Onof, C., Winter, H., 2020. Ensemble estimation of future rainfall extremes with  
524 temperature dependent censored simulation. *Adv. Water Resour.* 136, 103479.  
525 <https://doi.org/10.1016/j.advwatres.2019.103479>

526 Daloz, A.S., Camargo, S.J., 2018. Is the poleward migration of tropical cyclone maximum  
527 intensity associated with a poleward migration of tropical cyclone genesis? *Clim. Dyn.*  
528 50, 705–715. <https://doi.org/10.1007/s00382-017-3636-7>

529 Diffenbaugh, N.S., Singh, D., Mankin, J.S., Horton, D.E., Swain, D.L., Touma, D., Charland, A.,  
530 Liu, Y., Haugen, M., Tsiang, M., Rajaratnam, B., 2017. Quantifying the influence of  
531 global warming on unprecedented extreme climate events. *Proc. Natl. Acad. Sci.* 114,  
532 4881–4886. <https://doi.org/10.1073/pnas.1618082114>

533 Do, H.X., Westra, S., Leonard, M., 2017. A global-scale investigation of trends in annual  
534 maximum streamflow. *J. Hydrol.* 552, 28–43.  
535 <https://doi.org/10.1016/j.jhydrol.2017.06.015>

536 Donat, M.G., Alexander, L. V., Yang, H., Durre, I., Vose, R., Dunn, R.J.H., Willett, K.M., Aguilar,  
537 E., Brunet, M., Caesar, J., Hewitson, B., Jack, C., Klein Tank, a. M.G., Kruger, a. C.,  
538 Marengo, J., Peterson, T.C., Renom, M., Oria Rojas, C., Rusticucci, M., Salinger, J.,  
539 Elayah, a. S., Sekele, S.S., Srivastava, a. K., Trewin, B., Villarroel, C., Vincent, L. a., Zhai,  
540 P., Zhang, X., Kitching, S., 2013. Updated analyses of temperature and precipitation  
541 extreme indices since the beginning of the twentieth century: The HadEX2 dataset. *J.*  
542 *Geophys. Res. Atmos.* 118, 2098–2118. <https://doi.org/10.1002/jgrd.50150>

543 Emanuel, K., 2005. Increasing destructiveness of tropical cyclones over the past 30 years.  
544 Nature 436, 686–688. <https://doi.org/10.1038/nature03906>

545 Emmanuel, I., Andrieu, H., Leblois, E., Flahaut, B., 2012. Temporal and spatial variability of  
546 rainfall at the urban hydrological scale. J. Hydrol. 430–431, 162–172.  
547 <https://doi.org/10.1016/j.jhydrol.2012.02.013>

548 Fadhel, S., Rico-Ramirez, M.A., Han, D., 2018. Sensitivity of peak flow to the change of  
549 rainfall temporal pattern due to warmer climate. J. Hydrol. 560, 546–559.  
550 <https://doi.org/10.1016/j.jhydrol.2018.03.041>

551 Fowler, H.J., Lenderink, G., Prein, A.F., Westra, S., Allan, R.P., Ban, N., Barbero, R., Berg, P.,  
552 Blenkinsop, S., Do, H.X., Guerreiro, S., Haerter, J.O., Kendon, E.J., Lewis, E., Schaer, C.,  
553 Sharma, A., Villarini, G., Wasko, C., Zhang, X., 2021. Anthropogenic intensification of  
554 short-duration rainfall extremes. Nat. Rev. Earth Environ. 2, 107–122.  
555 <https://doi.org/10.1038/s43017-020-00128-6>

556 Frame, D.J., Wehner, M.F., Noy, I., Rosier, S.M., 2020. The economic costs of Hurricane  
557 Harvey attributable to climate change. Clim. Change 160, 271–281.  
558 <https://doi.org/10.1007/s10584-020-02692-8>

559 Gao, L., Tao, B., Miao, Y., Zhang, L., Song, X., Ren, W., He, L., Xu, X., 2019. A Global Data Set  
560 for Economic Losses of Extreme Hydrological Events During 1960–2014. Water Resour.  
561 Res. 55, 5165–5175. <https://doi.org/10.1029/2019WR025135>

562 Grise, K.M., Davis, S.M., Staten, P.W., Adam, O., 2018. Regional and seasonal characteristics  
563 of the recent expansion of the tropics. J. Clim. 31, 6839–6856.  
564 <https://doi.org/10.1175/JCLI-D-18-0060.1>

565 Guo, D., Thomas, J., Lazaro, A.B., Matwewe, F., Johnson, F., 2021. Modelling the influence of  
566 short-term climate variability on drinking water quality in tropical developing countries:  
567 A case study in Tanzania. Sci. Total Environ. 763, 142932.  
568 <https://doi.org/10.1016/j.scitotenv.2020.142932>

569 Haerter, J.O., Berg, P., 2009. Unexpected rise in extreme precipitation caused by a shift in  
570 rain type? Nat. Geosci. 2, 372–373. <https://doi.org/10.1038/ngeo523>

571 Hall, J., Arheimer, B., Borga, M., Brázdil, R., Claps, P., Kiss, A., Kjeldsen, T.R., Kriaučiūnienė, J.,  
572 Kundzewicz, Z.W., Lang, M., Llasat, M.C., Macdonald, N., McIntyre, N., Mediero, L.,  
573 Merz, B., Merz, R., Molnar, P., Montanari, A., Neuhold, C., Parajka, J., Perdigão, R.A.P.,  
574 Plavcová, L., Rogger, M., Salinas, J.L., Sauquet, E., Schär, C., Szolgay, J., Viglione, A.,

575 Blöschl, G., 2014. Understanding flood regime changes in Europe: a state-of-the-art  
576 assessment. *Hydrol. Earth Syst. Sci.* 18, 2735–2772. [https://doi.org/10.5194/hess-18-](https://doi.org/10.5194/hess-18-2735-2014)  
577 2735-2014

578 Hamed, K.H., 2009. Enhancing the effectiveness of prewhitening in trend analysis of  
579 hydrologic data. *J. Hydrol.* 368, 143–155. <https://doi.org/10.1016/j.jhydrol.2009.01.040>

580 Held, H., Gerstengarbe, F.W., Pardowitz, T., Pinto, J.G., Ulbrich, U., Born, K., Donat, M.G.,  
581 Karremann, M.K., Leckebusch, G.C., Ludwig, P., Nissen, K.M., Österle, H., Prah, B.F.,  
582 Werner, P.C., Befort, D.J., Burghoff, O., 2013. Projections of global warming-induced  
583 impacts on winter storm losses in the German private household sector. *Clim. Change*  
584 121, 195–207. <https://doi.org/10.1007/s10584-013-0872-7>

585 Hettiarachchi, S., Wasko, C., Sharma, A., 2018. Increase in flood risk resulting from climate  
586 change in a developed urban watershed – the role of storm temporal patterns. *Hydrol.*  
587 *Earth Syst. Sci.* 22, 2041–2056. <https://doi.org/10.5194/hess-22-2041-2018>

588 Hoeppe, P., 2016. Trends in weather related disasters – Consequences for insurers and  
589 society. *Weather Clim. Extrem.* 11, 70–79. <https://doi.org/10.1016/j.wace.2015.10.002>

590 IPCC, 2012. *Managing the Risks of Extreme Events and Disasters to Advance Climate Change*  
591 *Adaptation. A Special Report of Working Groups I and II of the Intergovernmental Panel*  
592 *on Climate Change.* Cambridge University Press, Cambridge.  
593 <https://doi.org/10.1017/CBO9781139177245>

594 Ivancic, T.J., Shaw, S.B., 2015. Examining why trends in very heavy precipitation should not  
595 be mistaken for trends in very high river discharge. *Clim. Change* 133, 681–693.  
596 <https://doi.org/10.1007/s10584-015-1476-1>

597 Jhajharia, D., Chattopadhyay, S., Choudhary, R.R., Dev, V., Singh, V.P., Lal, S., 2013. Influence  
598 of climate on incidences of malaria in the Thar Desert, northwest India. *Int. J. Climatol.*  
599 33, 312–325. <https://doi.org/10.1002/joc.3424>

600 Kalnay, E., Kanamitsu, M., Kistler, R., Collins, W., Deaven, D., Gandin, L., Iredell, M., Saha, S.,  
601 White, G., Woollen, J., Zhu, Y., Chelliah, M., Ebisuzaki, W., Higgins, W., Janowiak, J., Mo,  
602 K.C., Ropelewski, C., Wang, J., Leetmaa, A., Reynolds, R., Jenne, R., Joseph, D., 1996.  
603 The NCEP/NCAR 40-year reanalysis project. *Bull. Am. Meteorol. Soc.*  
604 [https://doi.org/10.1175/1520-0477\(1996\)077<0437:TNYRP>2.0.CO;2](https://doi.org/10.1175/1520-0477(1996)077<0437:TNYRP>2.0.CO;2)

605 Kay, A.L., Crooks, S.M., Pall, P., Stone, D.A., 2011. Attribution of Autumn/Winter 2000 flood  
606 risk in England to anthropogenic climate change: A catchment-based study. *J. Hydrol.*

607 406, 97–112. <https://doi.org/10.1016/j.jhydrol.2011.06.006>

608 Kendall, M., 1975. Rank correlation methods, 2nd Editio. ed. Griffin, London.

609 Kendall, M.G., 1938. A New Measure of Rank Correlation. *Biometrika* 30, 81.

610 <https://doi.org/10.2307/2332226>

611 Koenker, R., 2021. quantreg: Quantile Regression. R package version 5.85. [available at

612 <http://CRAN.R-project.org/package=quantreg>].

613 Koenker, R., Bassett, G., 1978. Regression Quantiles. *Econometrica* 46, 33–50.

614 <https://doi.org/10.2307/1913643>

615 Kron, W., Eichner, J., Kundzewicz, Z.W., 2019. Reduction of flood risk in Europe – Reflections

616 from a reinsurance perspective. *J. Hydrol.* 576, 197–209.

617 <https://doi.org/10.1016/j.jhydrol.2019.06.050>

618 Lenderink, G., Attema, J., 2015. A simple scaling approach to produce climate scenarios of

619 local precipitation extremes for the Netherlands. *Environ. Res. Lett.* 10, 085001.

620 <https://doi.org/10.1088/1748-9326/10/8/085001>

621 Lenderink, G., van Meijgaard, E., 2008. Increase in hourly precipitation extremes beyond

622 expectations from temperature changes. *Nat. Geosci.* 1, 511–514.

623 <https://doi.org/10.1038/ngeo262>

624 Li, C., Cheng, X., Li, N., Liang, Z., Wang, Y., Han, S., 2016. A Three-Parameter S-Shaped

625 Function of Flood Return Period and Damage. *Adv. Meteorol.* 2016, 1–11.

626 <https://doi.org/10.1155/2016/6583906>

627 Magan, B., Kim, S., Wasko, C., Barbero, R., Moron, V., Nathan, R., Sharma, A., 2020. Impact

628 of atmospheric circulation on the rainfall-temperature relationship in Australia.

629 *Environ. Res. Lett.* 15, 094098. <https://doi.org/10.1088/1748-9326/abab35>

630 Mallakpour, I., Villarini, G., 2015. The changing nature of flooding across the central United

631 States. *Nat. Clim. Chang.* 5, 250–254. <https://doi.org/10.1038/nclimate2516>

632 Martinez-Villalobos, C., Neelin, J.D., 2018. Shifts in Precipitation Accumulation Extremes

633 During the Warm Season Over the United States. *Geophys. Res. Lett.* 45, 8586–8595.

634 <https://doi.org/10.1029/2018GL078465>

635 Mathew, S.S., Kumar, K.K., 2019. Characterization of the long-term changes in moisture,

636 clouds and precipitation in the ascending and descending branches of the Hadley

637 Circulation. *J. Hydrol.* 570, 366–377. <https://doi.org/10.1016/j.jhydrol.2018.12.047>

638 McAneney, J., Sandercock, B., Crompton, R., Mortlock, T., Musulin, R., Pielke, R., Gissing, A.,

639 2019. Normalised insurance losses from Australian natural disasters: 1966–2017.  
640 Environ. Hazards 7891. <https://doi.org/10.1080/17477891.2019.1609406>

641 Mechler, R., Bouwer, L.M., 2015. Understanding trends and projections of disaster losses  
642 and climate change: is vulnerability the missing link? *Clim. Change* 133, 23–35.  
643 <https://doi.org/10.1007/s10584-014-1141-0>

644 Miller, J.D., Hutchins, M., 2017. The impacts of urbanisation and climate change on urban  
645 flooding and urban water quality: A review of the evidence concerning the United  
646 Kingdom. *J. Hydrol. Reg. Stud.* 12, 345–362. <https://doi.org/10.1016/j.ejrh.2017.06.006>

647 Miller, S., Muir-Wood, R., Boissonnade, A., 2008. An exploration of trends in normalized  
648 weather-related catastrophe losses, in: Diaz, H.F., Murnane, R.J. (Eds.), *Climate*  
649 *Extremes and Society*. Cambridge University Press, Cambridge, UK and New York, NY,  
650 USA, p. 340.

651 Mills, E., 2005. Insurance in a Climate of Change. *Science* (80-. ). 309, 1040–1044.  
652 <https://doi.org/10.1126/science.1112121>

653 Mills, E., Lecomte, E., Peara, A., 2002. Insurers in the Greenhouse. *J. Insur. Regul.* 21, 43–78.

654 Min, S.-K., Zhang, X., Zwiers, F.W., Hegerl, G.C., 2011. Human contribution to more-intense  
655 precipitation extremes. *Nature* 470, 378–81. <https://doi.org/10.1038/nature09763>

656 Molnar, P., Fatichi, S., Gaál, L., Szolgay, J., Burlando, P., 2015. Storm type effects on super  
657 Clausius–Clapeyron scaling of intense rainstorm properties with air temperature.  
658 *Hydrol. Earth Syst. Sci.* 19, 1753–1766. <https://doi.org/10.5194/hess-19-1753-2015>

659 Mondal, A., Mujumdar, P.P., 2015. Modeling non-stationarity in intensity, duration and  
660 frequency of extreme rainfall over India. *J. Hydrol.* 521, 217–231.  
661 <https://doi.org/10.1016/j.jhydrol.2014.11.071>

662 Munich RE, 2016. TOPICS GEO: Natural catastrophes 2015.

663 Myhre, G., Alterskjær, K., Stjern, C.W., Hodnebrog, Marelle, L., Samset, B.H., Sillmann, J.,  
664 Schaller, N., Fischer, E., Schulz, M., Stohl, A., 2019. Frequency of extreme precipitation  
665 increases extensively with event rareness under global warming. *Sci. Rep.* 9, 1–10.  
666 <https://doi.org/10.1038/s41598-019-52277-4>

667 NCEP, 1994. National Centers for Environmental Prediction/National Weather  
668 Service/NOAA/U.S. Department of Commerce. NCEP/NCAR Global Reanalysis Products,  
669 1948-continuing. Research Data Archive at NOAA/PSL:  
670 </data/gridded/data.ncep.reanalysis.html>.

671 Neukom, R., Barboza, L.A., Erb, M.P., Shi, F., Emile-Geay, J., Evans, M.N., Franke, J.,  
672 Kaufman, D.S., Lücke, L., Rehfeld, K., Schurer, A., Zhu, F., Brönnimann, S., Hakim, G.J.,  
673 Henley, B.J., Ljungqvist, F.C., McKay, N., Valler, V., von Gunten, L., 2019. Consistent  
674 multidecadal variability in global temperature reconstructions and simulations over the  
675 Common Era. *Nat. Geosci.* 12, 643–649. <https://doi.org/10.1038/s41561-019-0400-0>  
676 Neumayer, E., Barthel, F., 2011. Normalizing economic loss from natural disasters: A global  
677 analysis. *Glob. Environ. Chang.* 21, 13–24.  
678 <https://doi.org/10.1016/j.gloenvcha.2010.10.004>  
679 Nicholls, N., 2011. Comments on “Have disaster losses increased due to anthropogenic  
680 climate change?” *Bull. Am. Meteorol. Soc.* 92, 791–791.  
681 <https://doi.org/10.1175/2011BAMS3167.1>  
682 O’Gorman, P.A., 2015. Precipitation Extremes Under Climate Change. *Curr. Clim. Chang.*  
683 *Reports* 1, 49–59. <https://doi.org/10.1007/s40641-015-0009-3>  
684 Pall, P., Aina, T., Stone, D. a, Stott, P. a, Nozawa, T., Hilberts, A.G.J., Lohmann, D., Allen,  
685 M.R., 2011. Anthropogenic greenhouse gas contribution to flood risk in England and  
686 Wales in autumn 2000. *Nature* 470, 382–385. <https://doi.org/10.1038/nature09762>  
687 Paprotny, D., Sebastian, A., Morales-Nápoles, O., Jonkman, S.N., 2018. Trends in flood losses  
688 in Europe over the past 150 years. *Nat. Commun.* 9, 1985.  
689 <https://doi.org/10.1038/s41467-018-04253-1>  
690 Peleg, N., Marra, F., Fatichi, S., Molnar, P., Morin, E., Sharma, A., Burlando, P., 2018.  
691 Intensification of Convective Rain Cells at Warmer Temperatures Observed from High-  
692 Resolution Weather Radar Data. *J. Hydrometeorol.* 19, 715–726.  
693 <https://doi.org/10.1175/JHM-D-17-0158.1>  
694 Pielke, R.A., Gratz, J., Landsea, C.W., Collins, D., Saunders, M.A., Musulin, R., 2008.  
695 Normalized hurricane damage in the United States: 1900–2005. *Nat. Hazards Rev.* 9,  
696 29–42. [https://doi.org/10.1061/\(ASCE\)1527-6988\(2008\)9:1\(29\)](https://doi.org/10.1061/(ASCE)1527-6988(2008)9:1(29))  
697 Pielke, R.A., Landsea, C.N., 1999. La Nina, El Nino, and Atlantic Hurricane Damages in the  
698 United States. *Bull. Am. Meteorol. Soc.* 80, 2027–2033. [https://doi.org/10.1175/1520-0477\(1999\)080<2027:LNAENO>2.0.CO;2](https://doi.org/10.1175/1520-0477(1999)080<2027:LNAENO>2.0.CO;2)  
699  
700 Pielke, R.A., Rubiera, J., Landsea, C., Fernández, M.L., Klein, R., 2003. Hurricane Vulnerability  
701 in Latin America and The Caribbean: Normalized Damage and Loss Potentials. *Nat.*  
702 *Hazards Rev.* 4, 101–114. [https://doi.org/10.1061/\(ASCE\)1527-6988\(2003\)4:3\(101\)](https://doi.org/10.1061/(ASCE)1527-6988(2003)4:3(101))

703 Prein, A.F., Liu, C., Ikeda, K., Trier, S.B., Rasmussen, R.M., Holland, G.J., Clark, M.P., 2017.  
704 Increased rainfall volume from future convective storms in the US. *Nat. Clim. Chang.* 7,  
705 880–884. <https://doi.org/10.1038/s41558-017-0007-7>

706 Razavi, S., Gober, P., Maier, H.R., Brouwer, R., Wheeler, H., 2020. Anthropocene flooding:  
707 Challenges for science and society. *Hydrol. Process.* 34, 1996–2000.  
708 <https://doi.org/10.1002/hyp.13723>

709 Roderick, T.P., Wasko, C., Sharma, A., 2019. Atmospheric Moisture Measurements Explain  
710 Increases in Tropical Rainfall Extremes. *Geophys. Res. Lett.* 46, 1375–1382.  
711 <https://doi.org/10.1029/2018GL080833>

712 Rohde, R., Muller, R. a, Jacobsen, R., Perlmutter, S., Rosenfeld, A., Wurtele, J., Curry, J.,  
713 Wickham, C., Mosher, S., 2013. Berkeley Earth Temperature Averaging Process.  
714 *Geoinformatic Geostatistics An Overv.* 1, 1–13.  
715 <https://doi.org/http://dx.doi.org/10.4172/gigs.1000103>

716 Seidel, D.J., Fu, Q., Randel, W.J., Reichler, T.J., 2008. Widening of the tropical belt in a  
717 changing climate. *Nat. Geosci.* 1, 21–24. <https://doi.org/10.1038/ngeo.2007.38>

718 Seneviratne, S., Nicholls, N., Easterling, D., Goodess, C., Kanae, S., Kossin, J., Luo, Y.,  
719 Marengo, J., McInnes, K., Rahimi, M., Reichstein, M., Sorteberg, A., Vera, C., Zhang, X.,  
720 2012. Changes in climate extremes and their impacts on the natural physical  
721 environment, in: Field, C.B., Barros, V., Stocker, T.F., Qin, D., Dokken, D.J., Ebi, K.L.,  
722 Mastrandrea, M.D., Mach, K.J., Plattner, G.-K., Allen, S.K., Tignor, M., Midgley, P.M.  
723 (Eds.), *Managing the Risk of Extreme Events and Disasters to Advance Climate Change*  
724 *Adaptation*. Cambridge University Press, A Special Report of Working Groups I and II of  
725 the Intergovernmental Panel on Climate Change (IPCC). Cambridge, UK, and New York,  
726 NY, USA, pp. 109–230.

727 Sharma, A., Wasko, C., Lettenmaier, D.P., 2018. If Precipitation Extremes Are Increasing,  
728 Why Aren't Floods? *Water Resour. Res.* 54, 8545–8551.  
729 <https://doi.org/10.1029/2018WR023749>

730 Slater, L., Villarini, G., Archfield, S., Faulkner, D., Lamb, R., Khouakhi, A., Yin, J., 2021. Global  
731 Changes in 20-Year, 50-Year, and 100-Year River Floods. *Geophys. Res. Lett.* 48, 1–10.  
732 <https://doi.org/10.1029/2020GL091824>

733 Staten, P.W., Lu, J., Grise, K.M., Davis, S.M., Birner, T., 2018. Re-examining tropical  
734 expansion. *Nat. Clim. Chang.* 8, 768–775. <https://doi.org/10.1038/s41558-018-0246-2>

735 Sun, Q., Zhang, X., Zwiers, F., Westra, S., Alexander, L. V., 2021. A Global, Continental, and  
736 Regional Analysis of Changes in Extreme Precipitation. *J. Clim.* 34, 243–258.  
737 <https://doi.org/10.1175/JCLI-D-19-0892.1>

738 SwissRe, 2016. *Sigma. Natural Catastrophes and Man-Made Disasters.*

739 Towler, E., Rajagopalan, B., Gilleland, E., Summers, R.S., Yates, D., Katz, R.W., 2010.  
740 Modeling hydrologic and water quality extremes in a changing climate: A statistical  
741 approach based on extreme value theory. *Water Resour. Res.* 46, W11504.  
742 <https://doi.org/10.1029/2009WR008876>

743 Trambly, Y., Mimeau, L., Neppel, L., Vinet, F., Sauquet, E., 2019. Detection and attribution  
744 of flood trends in Mediterranean basins. *Hydrol. Earth Syst. Sci.* 23, 4419–4431.  
745 <https://doi.org/10.5194/hess-23-4419-2019>

746 Trenberth, K.E., 2011. Changes in precipitation with climate change. *Clim. Res.* 47, 123–138.  
747 <https://doi.org/10.3354/cr00953>

748 Trenberth, K.E., Dai, A., Rasmussen, R.M., Parsons, D.B., 2003. The changing character of  
749 precipitation. *Bull. Am. Meteorol. Soc.* 84, 1205–1217. [https://doi.org/10.1175/BAMS-](https://doi.org/10.1175/BAMS-84-9-1205)  
750 [84-9-1205](https://doi.org/10.1175/BAMS-84-9-1205)

751 UN, 2017. United Nations National Accounts Main Aggregates Database [WWW Document].  
752 URL <https://unstats.un.org/unsd/snaama/dnList.asp>

753 van Oldenborgh, G.J., van der Wiel, K., Sebastian, A., Singh, R., Arrighi, J., Otto, F., Haustein,  
754 K., Li, S., Vecchi, G., Cullen, H., 2017. Attribution of extreme rainfall from Hurricane  
755 Harvey, August 2017. *Environ. Res. Lett.* 12, 124009. [https://doi.org/10.1088/1748-](https://doi.org/10.1088/1748-9326/aa9ef2)  
756 [9326/aa9ef2](https://doi.org/10.1088/1748-9326/aa9ef2)

757 Wasko, C., 2021. Review: Can temperature be used to inform changes to flood extremes  
758 with global warming? *Philos. Trans. R. Soc. A Math. Phys. Eng. Sci.* 379, 20190551.  
759 <https://doi.org/10.1098/rsta.2019.0551>

760 Wasko, C., Nathan, R., 2019. Influence of changes in rainfall and soil moisture on trends in  
761 flooding. *J. Hydrol.* 575, 432–441. <https://doi.org/10.1016/j.jhydrol.2019.05.054>

762 Wasko, C., Sharma, A., 2017a. Continuous rainfall generation for a warmer climate using  
763 observed temperature sensitivities. *J. Hydrol.* 544, 575–590.  
764 <https://doi.org/10.1016/j.jhydrol.2016.12.002>

765 Wasko, C., Sharma, A., 2017b. Global assessment of flood and storm extremes with  
766 increased temperatures. *Sci. Rep.* 7, 7945. <https://doi.org/10.1038/s41598-017-08481->

767 1

768 Wasko, C., Sharma, A., 2015. Steeper temporal distribution of rain intensity at higher  
769 temperatures within Australian storms. *Nat. Geosci.* 8, 527–529.

770 <https://doi.org/10.1038/ngeo2456>

771 Wasko, C., Sharma, A., 2014. Quantile regression for investigating scaling of extreme  
772 precipitation with temperature. *Water Resour. Res.* 50, 3608–3614.

773 <https://doi.org/10.1002/2013WR015194>

774 Wasko, C., Sharma, A., Johnson, F., 2015. Does storm duration modulate the extreme  
775 precipitation-temperature scaling relationship? *Geophys. Res. Lett.* 42, 8783–8790.

776 <https://doi.org/10.1002/2015GL066274>

777 Wasko, C., Sharma, A., Lettenmaier, D.P., 2019. Increases in temperature do not translate to  
778 increased flooding. *Nat. Commun.* 10, 5676. [https://doi.org/10.1038/s41467-019-](https://doi.org/10.1038/s41467-019-13612-5)

779 13612-5

780 Webster, P.J., 2005. Changes in Tropical Cyclone Number, Duration, and Intensity in a  
781 Warming Environment. *Science* (80-. ). 309, 1844–1846.

782 <https://doi.org/10.1126/science.1116448>

783 Weinkle, J., Landsea, C., Collins, D., Musulin, R., Crompton, R.P., Klotzbach, P.J., Pielke, R.,  
784 2018. Normalized hurricane damage in the continental United States 1900–2017. *Nat.*

785 *Sustain.* 1, 808–813. <https://doi.org/10.1038/s41893-018-0165-2>

786 Welker, C., Faust, E., 2013. Tropical cyclone-related socio-economic losses in the western  
787 North Pacific region. *Nat. Hazards Earth Syst. Sci.* 13, 115–124.

788 <https://doi.org/10.5194/nhess-13-115-2013>

789 Westra, S., Alexander, L., Zwiers, F., 2013a. Global increasing trends in annual maximum  
790 daily precipitation. *J. Clim.* 26, 3904–3918.

791 <https://doi.org/http://dx.doi.org/10.1175/JCLI-D-12-00502.1>

792 Westra, S., Evans, J.P., Mehrotra, R., Sharma, A., 2013b. A conditional disaggregation  
793 algorithm for generating fine time-scale rainfall data in a warmer climate. *J. Hydrol.*

794 479, 86–99. <https://doi.org/10.1016/j.jhydrol.2012.11.033>

795 Westra, S., Fowler, H.J., Evans, J.P., Alexander, L., Berg, P., Johnson, F., Kendon, E.J.,

796 Lenderink, G., Roberts, N.M., 2014. Future changes to the intensity and frequency of  
797 short-duration extreme rainfall. *Rev. Geophys.* 52, 522–555.

798 <https://doi.org/10.1002/2014RG000464>

799 Zamani, R., Mirabbasi, R., Abdollahi, S., Jhajharia, D., 2017. Streamflow trend analysis by  
800 considering autocorrelation structure, long-term persistence, and Hurst coefficient in a  
801 semi-arid region of Iran. *Theor. Appl. Climatol.* 129, 33–45.  
802 <https://doi.org/10.1007/s00704-016-1747-4>

803 Zhang, W., Villarini, G., Wehner, M., 2019. Contrasting the responses of extreme  
804 precipitation to changes in surface air and dew point temperatures. *Clim. Change.*  
805 <https://doi.org/10.1007/s10584-019-02415-8>

806 Zhang, X., Zwiers, F.W., Li, G., Wan, H., Cannon, A.J., 2017. Complexity in estimating past and  
807 future extreme short-duration rainfall. *Nat. Geosci.* 10, 255–259.  
808 <https://doi.org/10.1038/ngeo2911>

809  
810